INDRA/COV: A NEW TOOL FOR OPTIMIZATION OF CONSTELLATIONS COVERAGE STATISTICS[1]

Conrad SCHIFF
Laurie MAILHE

a.i. solutions, Inc.
10001 Derekwood Lane, Suite 215
Lanham, MD 20706 USA
(301) 306-1756
FAX: (301) 306-1754
(schiff@ai-solutions.com)
(mailhe@ai-solutions.com)
(301) 306-1756
FAX: (301) 306-1754

ABSTRACT *A new constellation design, proposed by the Global Precipitation Measurement (GPM) mission, relies on a combination of dedicated and shared resources in order to provide accurate continuous rainfall measurement. We discuss the challenge of understanding and designing orbits for the dedicated resources so that they complement the coverage obtained from the shared resources. We begin by presenting the GPM hybrid constellation concept along with our proposed analysis methods and constellation metrics. We then discuss the evolution of our tools from our standalone prototype, named Indra/COV, to a fully developed model in FreeFlyer. We finish with a discussion of the results produced by both tools, our conclusions, and our goals for future work.*

KEYWORDS: Constellation Design, Coverage, Optimization, Visualization.

INTRODUCTION

Reducing mission cost by sharing resources is a concept increasingly embraced by the civilian space industry. A new constellation design for the Global Precipitation Measurement (GPM) mission relies heavily on this concept. A primary GPM objective is 'to provide frequent sampling of rainfall measurement to reduce the uncertainty in estimating global Earth rainfall accumulation'[1]. This accuracy can only be achieved by using a constellation of spacecraft. To satisfy this requirement in a cost-effective manner, the GPM project envisions using resources from already or soon-to-be launched satellites with suitable instruments (radiometers) for rainfall measurement. Those spacecraft are referred as "Fixed" spacecraft in this paper. Designed for separate mission goals, they have predetermined orbital elements, instruments, and groundtrack behavior, which cannot be changed for GPM purpose. In addition

[1] This work was performed under NASA/GSFC contract NAS5-01090, task 64.

to the fixed spacecraft, the GPM project will supply its own satellites, referred to here as "Varied" or "Drone" spacecraft. The Varied spacecraft will complement the coverage obtained by the Fixed spacecraft orbit so that the science requirements are satisfied. While this new concept saves a major part of the budget that would be allocated for building, launching and monitoring each of the Fixed spacecraft, it also raises new challenges. As mentioned earlier, these Fixed spacecraft all have different orbital elements, instruments, and groundtrack evolutions. The constellation that results from combining them with the Varied spacecraft becomes very hard to analyze. Broadly speaking, three main analysis areas must be explored before the mission design can move to the operational phases. First of all, there is the initial placement of the Varied spacecraft so as to best complement the Fixed spacecraft. Then the issues associated with long-term stability (i.e. yearly evolution of the selected performance index) and maintenance must be explored. Finally, consideration of performance plateaus and graceful degradation in the GPM constellation must be made since each satellite will generally have different launch dates and orbital lifetimes. The resulting effect is that the GPM constellation will be adding or losing spacecraft during its operational life.

This paper presents our preliminary efforts in dealing with the complexity presented by the GPM hybrid-constellation. For the most part, we have focused our analysis on the first point listed above, namely determining the placement of the Varied spacecraft. However, some of our analysis touches on the other two points and will be discussed in turn. In the first section of this work, we define the various coverage metrics employed. The second section focuses on the evolution of our coverage tools. We first present a description of the Matlab standalone tool named Indra/COV, which we developed as a quick prototype to enable us to gain insight into what is a good figure of merit for the mission. Much of our intuition was derived from our interaction with the Indra/COV and thus a discussion of the tool is vital. We next discuss those major features of Indra/COV which were then implemented in FreeFlyer. This step was done to alleviate the computational limitations in Indra/COV. In the next section we deal with the results obtained in combination from both tools. We conclude with a discussion of the future directions in our analysis. In particular, we examine some of the limitations in our current analysis and suggest how our current results, obtained using a genetic algorithm (GA), might remedy these shortcomings.

GPM COVERAGE CONCEPT AND FIGURES-OF-MERIT

Coverage Points

Before any discussion can be made of mission figure-of-merits and their various pros and cons, an adequate definition of coverage must be adopted. While it is fairly common to deal with a definition of constellation coverage that accounts for overlapping conical fields-of-view projected onto a spherical Earth from spacecraft in essentially circular orbit (e.g. [2]), this approach becomes difficult to extend to complex sensors viewing an ellipsoidal Earth from arbitrary orbits. As a result, we adopted a different approach. We assumed that the coverage could be obtained from a sufficiently dense set of coverage points that effectively cover the Earth's surface. If a constellation can see each of the points at least once within its sensor's field-of view for a given duration, we then assumed that it has seen the entire Earth's surface. This approach requires a distribution method that places points in approximately equal area regions at both the equator and the poles. Two distribution methods were initially implemented. The first method [3] we dubbed the 'Helical Distribution' because the distribution of points looked much like what is obtained by pealing an orange in one piece. The second method [4] we dubbed the 'Symmetric Method' because it balanced a point in one location by the placement of a point in the antipodal location. The number of points used in the distribution will be denoted hereafter as N_{cov}. Figure 1 shows the placement of $N_{cov} = 500$ points for both distributions.

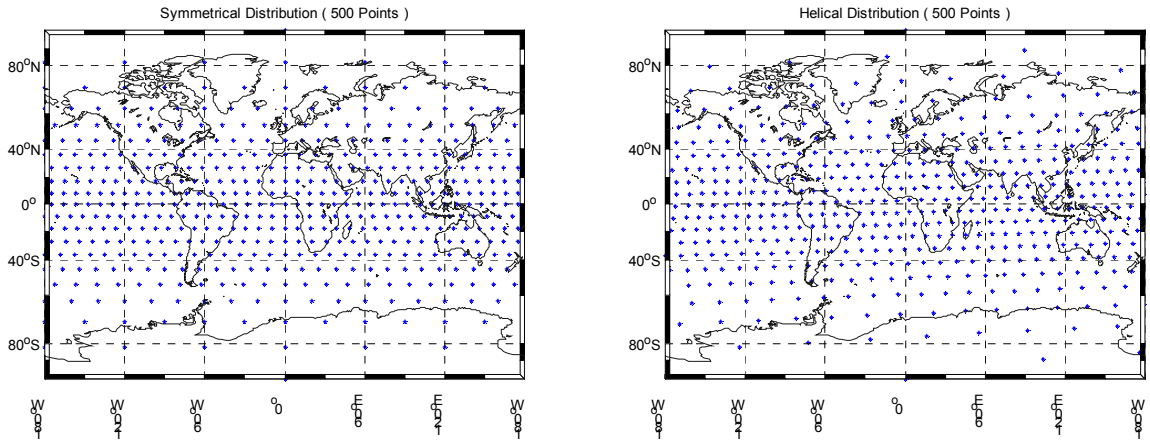

Fig. 1. Symmetrical (Left) and Helical (Right) Distributions with 500 Points.

Figures of Merits

Once the points are distributed, a variety of figures-of-merit can be defined. Since we currently do not have a science-derived figure-of-merit we explored three different ones during our analysis of the GPM constellation; 1) Coverage, 2) Revisit Statistics, and 3) Binning Statistics.

To define the first figure-of-merit, Coverage, start by assigning a logical variable, initialized to zero (meaning *not seen*) to each of the N_{cov} points. If during any time step of the constellation's propagation period a given point falls within a sensor footprint, the value of the logical variable is set to one (meaning *seen*). Once a given point has been seen, subsequent viewing are ignored for the duration of the coverage measurement. As mentioned in the Introduction, the basic period of time driven by the GPM science requirements is 3 hours. Based on the sensor characteristics (to be given below), we propagated the constellation at 60-second steps. Note that the step size was carefully chosen to generate a continuous swath while keeping the computational burden to a minimum. Figure 2 shows a typical spatial distribution of points. The points, which were seen at least once, are set to clear and the points that remained unseen are colored blue so that the gaps between the swaths of the constellation spacecraft are more obvious to the eye.

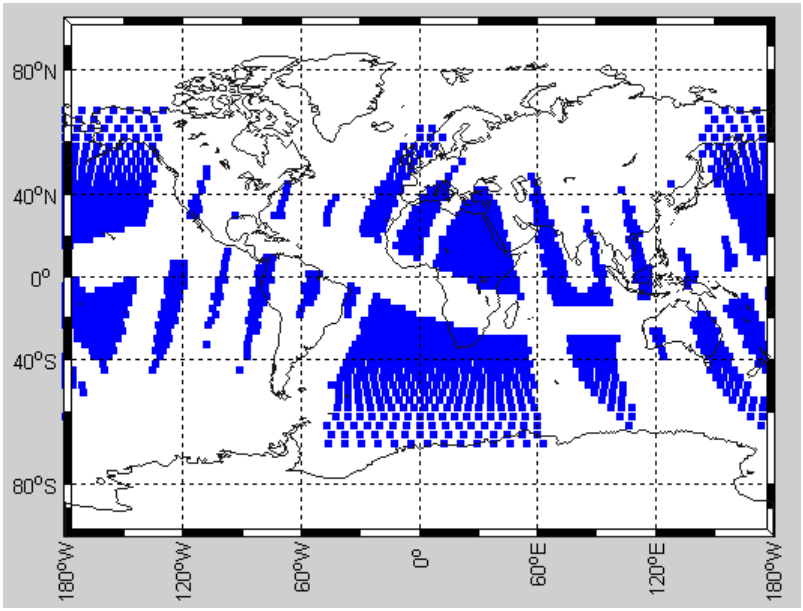

Fig. 2. A Sample Visualization Plot of the Coverage Figure-of-Merit.

Of course, the visualization shown in Figure 2, while compelling to the human eye, is hard to characterize for optimization purposes. In this latter case, a spatial averaging of the Coverage figure-of-merit is easily obtained. This spatial average is referred to as the Percent Coverage and is defined as the ratio of the points seen to the total number of points, N_{cov}.

The next figure-of-merit defined, the Revisit Statistics, attempts to take into account the continuous fluctuation in the Coverage figure-of-merit by tracking how often a point is revisited during the propagation period of the constellation. A *revisit* is defined to be the elapsed time between when a given point first enters a sensor's field-of-view and when the same point again enters a sensor field-of-view. While a point may be revisited by the same spacecraft or different spacecraft in succession, care is taken to ensure that the Revisit Statistics do not over-count the revisits. If a point is seen during multiple subsequent time steps as a sensor footprint moves across the surface of the Earth, only one revisit is recorded. Using the revisit as a basic unit various related statistics can be accumulated. Of the possible choices, we kept five related Revisit Statistics for each of the N_{cov} points: 1) the Number of Revisits, 2) the Average Revisit Time, 3) the Worst Revisit Time, 4) the Best Revisit Time, and 5) the Standard Deviation in the Average Revisit Time. The Number of Revisits is defined as the number of times a point on the Earth has been seen during the duration of the run. The Average Revisit Time records the average of all the revisit times for a given point whereas the worst and the best revisits time report respectively the longer revisit time and the shorter revisit time for a given point. Finally, to get a better understanding of the fluctuation over time of the Average Revisit Time, we record its temporal standard deviation. Figure 3 shows a sample plot for the Number of Revisit for each of N_{cov} = 5000 points gathered over 7 days. Again, the human eye can easily pick out patterns that suggest avenues for improvement and further study, but for the optimization, use of a spatial average was made.

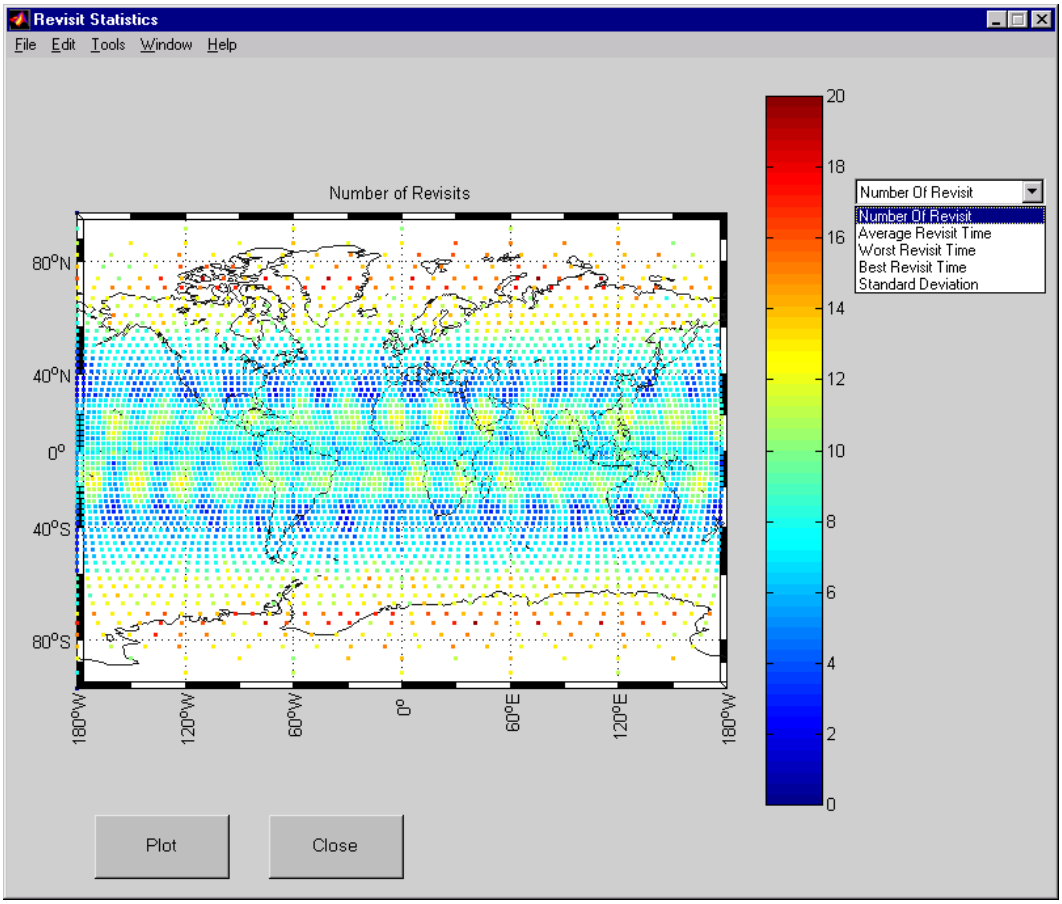

Fig. 3. A Sample Visualization Plot of the Revisit Statistics Figure-of-Merit Showing the Number of Revisits for Each Point

The final figure-of-merit, Binning Statistics, is a hybrid measurement that attempts to capture the flavor of the Revisit Statistics (in particular the Number of Revisits and the Average Revisit Time) without incurring the computational burden. It is based on the Coverage figure-of-merit but extends the concept to long time measurements. Each day is divided into 8 'time-bins', each bin being 3 hours in duration. The Coverage figure-of-merit is then kept for each of the N_{cov} points for each 'time-bin' in the propagation duration. Temporal averaging of the results then yields the desired Binning Statistics. To be concrete, consider a 7-day propagation of the constellation. Since, each day consists of 8 'time-bins', there are a maximum of 56 possible 'hits' for each of the N_{cov} points. Dividing the actual number of 'hits' by the total number of 'time-bins' gives a ratio that estimates how often a point is seen during the 7-day span and what the average revisit time is (to within a rough granularity). The resulting visuals are similar to the Revisit Statistics shown in Figure 3 and since they will be dealt with in detail below are not shown here. Like the other figure-of-merits, Binning Statistics can be spatially averaged for use in optimizing.

We close this section with Figure 4, which schematically shows the relationship between the three figure-of-merits discussed above.

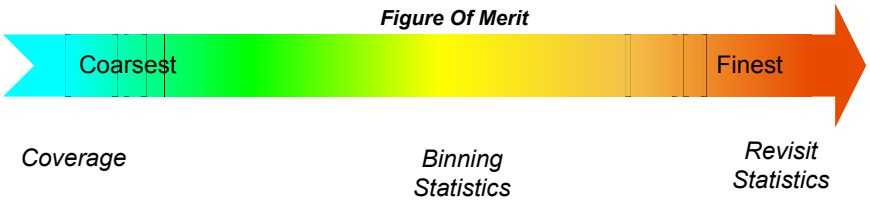

Fig. 4. A Schematic Comparison of the Three Figures-of-Merit Discussed in the Text. Note that as the level of details generated by the different figure-of-merit increases, the computing performance decreases.

EVOLUTION OF THE COVERAGE TOOLS

In this section we discuss the evolution of the coverage tools. Our reason for this two-fold. First we would like to introduce some functionality that we have developed for use in GPM that we believe is essentially new. Secondly, our analysis approach has grown as our tool set has evolved and we believe we would be doing a disservice by omitting the insight that was obtained. We begin with a discussion of our original prototype, Indra/COV, and finish with a presentation of the ***FreeFlyer®***/Matlab® solution that we are currently using.

Standalone Prototype : Indra/COV

Indra/COV is standalone tool written in entirely in Matlab for analyzing and visualizing different constellation configurations in terms of coverage figures-of-merit detailed above. As discussed above, it was developed for the Global Precipitation Measurement (GPM) mission out of the NASA Goddard Space Flight Center, Flight Analysis and Dynamics Branch. Our aim in developing Indra/COV was to provide a prototype environment in which various figures-of-merit, methods of visualization and optimization techniques could be rapidly implemented and analyzed.

When launched from Matlab, the Indra/COV GUI is spawned, resulting in a Matlab figure that looks like Figure 5. Each of the functional areas will be discussed briefly.

Functional area 1 contains the Load/Save Functionality. Using the Load and Save buttons, the user can either restore a previously created constellation and the accompanying results or save the current configuration. The data is retrieved and written in the Matlab workspace format.

Functional area 2 contains the Constellation Definition and Analysis Functionality. In this portion of the GUI, the user defines the parameters related to the N_{cov} points distributed on the Earth's surface. These parameters include the number of desired points, the method used to distribute them, any latitude restrictions, and the granularity of a subsidiary coverage grid that allows for fast hierarchical scanning through the points during each time step. The user also defines the propagation duration, time step, and force model (the choices being between two-body and J2 propagation). In addition, the user specifies the the spacecraft that make-up the constellation, including in these specifications whether the spacecraft are to be regarded as Fixed spacecraft (see the Introduction) or Varied spacecraft whose orbital elements can be changed by the optimizer.

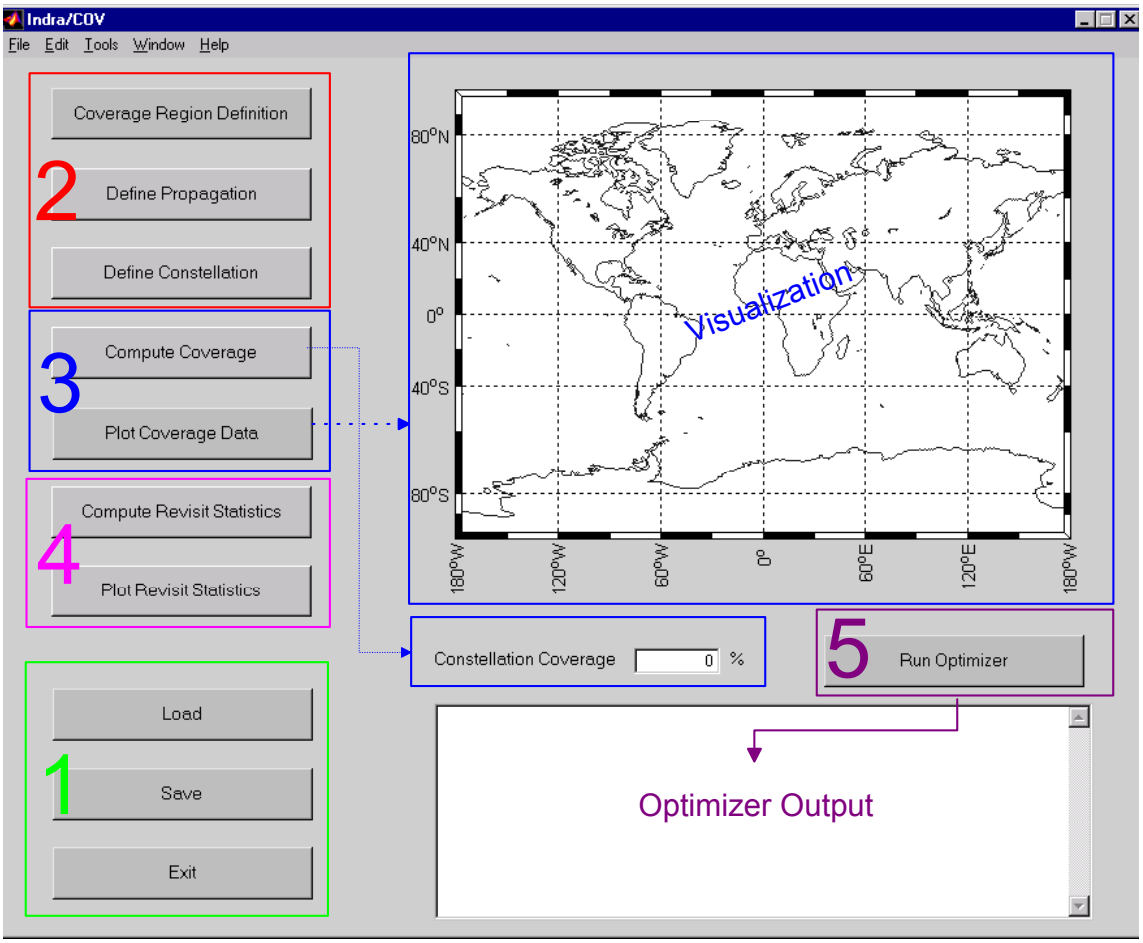

Fig. 5. Indra/COV Start Screen. Each functionality group is discussed below in the order referred by its number.

Figures 6 and 7 show the main dialogs used for defining the constellation. The first dialog (Figure 6) exhibits all the spacecraft that already compose the existing constellation. From this panel, the user can delete, access and edit information about each individual existing spacecraft or add a new spacecraft to the constellation by clicking on <new> entry.

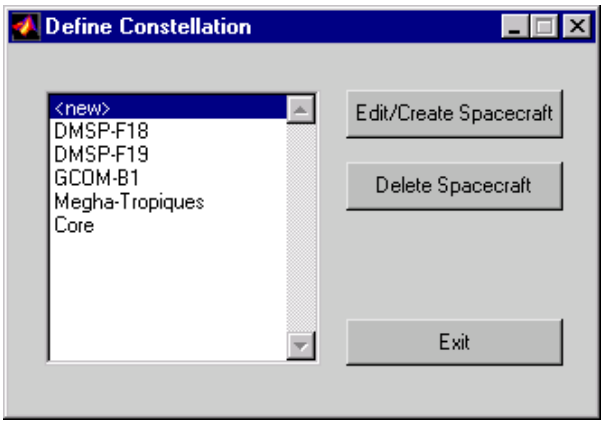

Fig. 6. Define Constellation Panel

Figure 7 shows the dialog that is spawned when a spacecraft is created or edited. For each satellite, the user can define its orbital elements as altitude, eccentricity, inclination, right ascension of the ascending node, argument of perigee and true anomaly. Each of these elements can be flagged so that it may be varied by the optimizer. On this panel, the user also defines the sensor parameter as swath width for a given altitude.

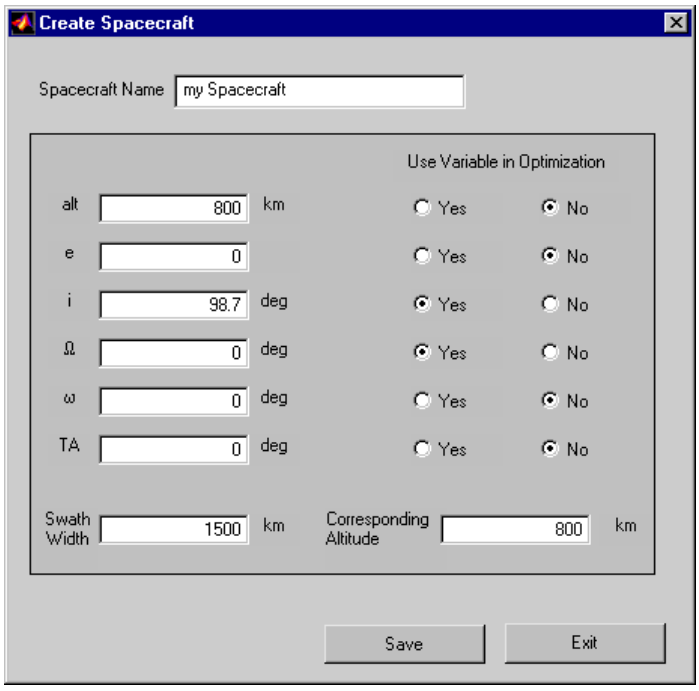

Fig. 7. Create Spacecraft Panel

Functional areas 3 and 4 form the visualization and analysis portions of Indra/COV. Once the coverage region is defined, the propagation and the constellation are initialized, the user can compute the Coverage and Revisit Statistics figures-of-merit[2] and visualize the results in these regions. All of the visualizations

[2] A beta-version of Indra/COV currently exists which also implements the Binning Statistics figure-of-merit. Currently there are no plans to release this version.

shown in this paper are done using the M_map a freeware package [5] available for Matlab. Figures 3 and 4 were produced in Indra/COV using M_map.

The final functional area is area 5, which comprises the optimizing portion of Indra/COV. The optimization is done via the Matlab Optimization ToolBox using a modified form of fmincon. In the current release of Indra/COV, only the Coverage figure-of-merit is used as the objective function.

Recognizing the need for flexibility, Indra/COV allows the figures-of-merit to visualized and computed for various combinations of spacecraft comprising the constellation for both the initialized set of spacecraft and the set obtained by an optimizer. This functionality allowed us to play out a variety of trade-off studies and is a paradigm that we followed when we moved beyond the prototype stage.

FreeFlyer/Matlab Solution

As experience was gained with Indra/COV it became apparent that its fundamental limitation was the computational performance that was obtained using Matlab. The decision was then made to move the analysis into a higher performance environment. However, we needed to ensure that the good features of Indra/COV were preserved. These considerations led us to an implementation of the core calculations in FreeFlyer supplemented with data post-processing and visualization in Matlab. This implementation allows access to the high-fidelity, full object-oriented functionality of FreeFlyer. In particular, FreeFlyer's ability to propagate multiple spacecraft simultaneously provided a natural solution to the placement problem of the Varied or Drone spacecraft with respect to the Fixed.

RESULTS

This section details our current results for the GPM analysis. We begin by presenting the results obtained with Indra/COV. Visual plots of the Binning Statistics for each coverage point mostly comprise these results. We then present the results obtained from the FreeFlyer/Matlab solution. The bulk of these results are based on spatial averages of the Binning Statistics figure-of-merit. Recall that the Binning Statistics are defined as the ratio of number of bin hit to the total number of bins for a given run. Each day is divided into 8 'time-bins', each bin being 3 hours in duration. In general, the visual plots provide a richer representation than the spatial averages but are not amenable to automation or optimization. We finish by discussing some preliminary work that has been performed with Genetic Algorithms, which we hope will begin to bridge the two approaches.

Indra/COV Results

Coverage and Optimization

In this section, we present one example of the results obtained using a modified fmincon to optimize a 3-hour coverage in Indra/COV. We looked into a constellation of 8 spacecraft. The first 5 spacecraft comprised the Fixed and consisted of DMSP-F18, DMSP-F19, GCOMB1, GPM-Core, and Megha-Tropiques. Their orbital elements are given in Table 1.

Table 1. Fixed Spacecraft Orbital Elements.

Orbital Element or Parameter	DMSP-F18	DMSP-F19	Megha-Tropiques	GPM-Core	GCOMB1
alt (km)	833	833	867	400	803
e	0	0	0	0	0
i (deg)	98.748	98.748	22	65	98.620
Ω (deg)	152.03	197.03	263.32	69.25	227.28

ω (deg)	0	0	0	0	0
f (deg)	0	0	0	0	0
swath width (km)	1707	1707	1600	920	1600
swath alt. (km)	833	833	800	400	803
half-angle (deg)[3]	43.715	43.715	43.186	47.811	43.085

The inclination and node of the 3 remaining spacecraft were varied to optimize coverage. The optimizer converged to an 85.65%-coverage with the following constellation orbital elements:

Table 2. Orbital Element of the Optimized Constellation Coverage Using fmincon

Orbital Element or Parameter	Drone 1	Drone 2	Drone3
alt (km)	600	600	600
e	0	0	0
i (deg)	87.76	35.89	74.92
Ω (deg)	286.33	232.2	71.30
ω (deg)	0	0	0
f (deg)	0	0	0
swath width (km)	1600	1600	1600
swath alt. (km)	800	800	800
half-angle (deg)[4]	43.186	43.186	43.186

However, this result only characterizes an instantaneous 3-hour coverage. To capture the temporal variation of this 3-hour coverage, we introduce Binning Statistics as our new figure-of-merit. Note that using fmincon with Binning Statistics would be computationally too long as one 3-hour coverage optimization run takes about 1 hour.

Binning Statistics

This section attempts to determine the run period necessary to obtain a significant and stable figure-of-merit. Figure 8 shows spatial snapshots every 2 days of average Binning Statistics over a period of 15 days. We notice that after about 8 to 9 Days the spatial average Binning Statistics hardly change. Thus, for this preliminary study, we chose run periods of 7 days and 15 days.

[3] The half-angle value is not independent of the swath width and swath altitude values. Rather it represents an ideal conical sensor that was used in place of the true complex sensor footprint in Indra/COV. For consistency, this simplification was also used in our FreeFlyer analysis. Future work will include the true sensor footprints.

[4] At the time of this writing, the sensor complement of the Drones was not determined and the values from Megha-Tropiques were used.

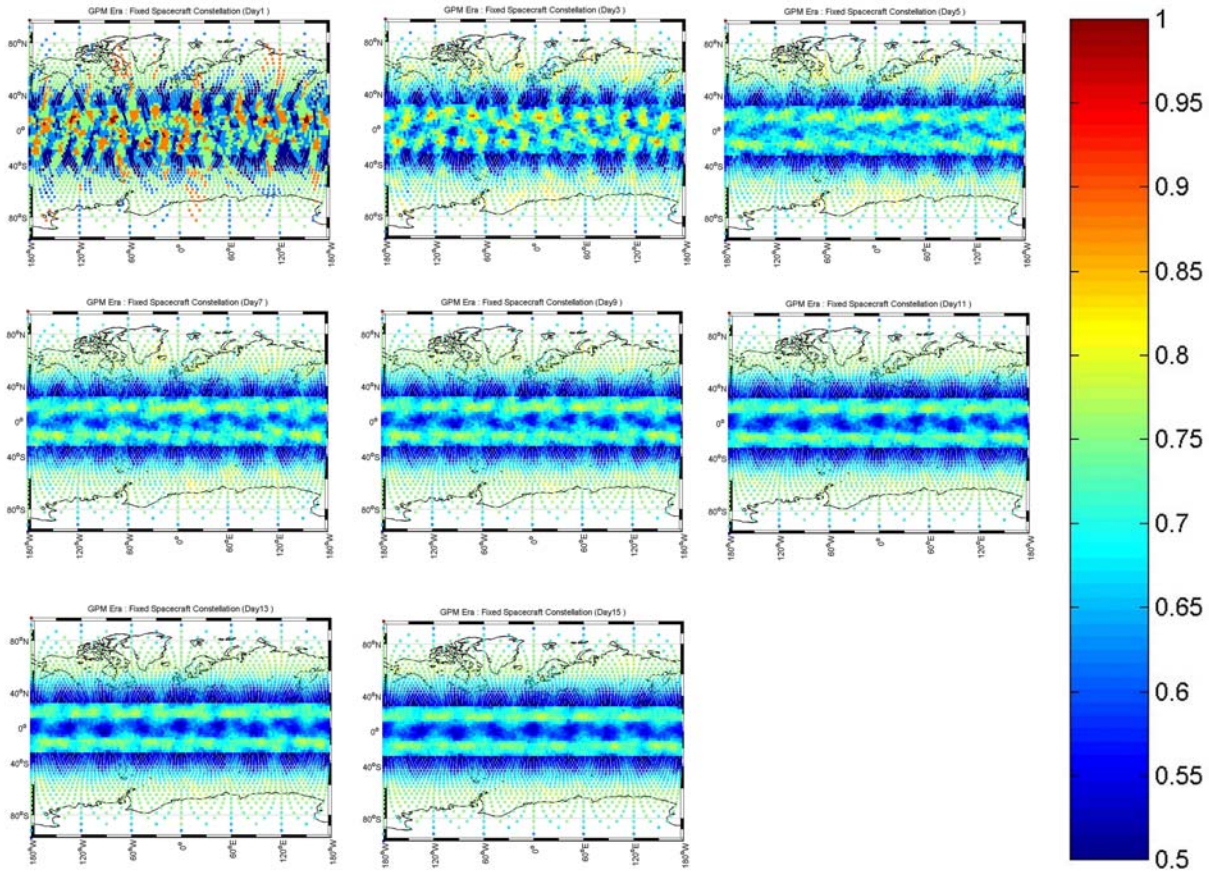

Fig. 8. 15-Day Average Binning Statistics Spatial Evolution.

FreeFlyer/Matlab Results

Arbitrary Drones

Using ***FreeFlyer®,*** 47 spacecraft were propagated for 15 days with a 60-second step size using a J_2 force-model. Separate Binning Statistics were kept for each spacecraft over each of the 15 days, with 8 bins per day, giving a total of 120 bins. The number of points used in the coverage model was 5000. The data was generated in *FreeFlyer®*, in approximately 2.5 hours, and was collected in Matlab®. The resulting data was just over 215 megabytes.

The 47 spacecraft fell into two classes. The first 5 spacecraft comprised the Fixed and their orbital elements were given in Table 1. The remaining 42 spacecraft were termed the Drones. Each Drone was given the same starting altitude, eccentricity, argument of perigee, and true anomaly. These are given in Table 3. In addition, the Drones were assigned a cone half-angle of 43.2°.

Table 3. Orbital Elements Common to All Drone Spacecraft.

Drone Orbital Element	Value
alt.	600 km
e	0
ω	0°
f	0°

The Drones inclination and right-ascension of the ascending node were varied as follows. Seven different inclinations were chosen ranging from 35 to 95 degrees in steps of 10 degrees. For each inclination, the right-ascension of the ascending nodes ranged from 0 to 150 degrees in steps of 30 degrees, ensuring that a node (either ascending or descending) was found every 30 degrees. This approach is summarized in Table 4.

Table 4. Schematic Representation of the GPM Scanning Analysis. The numbers in the cells are a short-hand for the Drone spacecraft. Thus, Drone25 has an inclination of 75° and a right-ascension of ascending node of 0°.

inc	Ω = 0°	Ω = 30°	Ω = 60°	Ω = 90°	Ω = 120°	Ω = 150°
35°	1	2	3	4	5	6
45°	7	8	9	10	11	12
55°	13	14	15	16	17	18
65°	19	20	21	22	23	24
75°	25	26	27	28	29	30
85°	31	32	33	34	35	36
95°	37	38	39	40	41	42

Once the ***FreeFlyer®*** run was completed, different GPM constellation configurations were examined. Each constellation consisted of the 5 Fixed spacecraft plus between 1 and 5 Drones. Because of the computationally intense nature of the scanning and the combinatorial explosion that results for large number of spacecraft in the constellation, not all possible combinations were analyzed. As mentioned above, current work is underway to determine if a Genetic Algorithm can help handle this complexity. Table 5 shows the type of constellation and the number of cases examined.

Table 5. GPM Constellation Runs

Constellation Type	Number of Possible Cases	Number of Examined Cases	Approximate Computing Time (PII 500MHz)
Fixed + 1 Drone	42	42	1 min
Fixed + 2 Drones	861	861	20 min
Fixed + 3 Drones	11480	1330	30 min
Fixed + 4 Drones	111930	5985	2 hours 15 min
Fixed + 5 Drones	850668	20349	8 hours 30 min

In order to make the results more manageable, the spatial average of the Binning Statistics were generated in a set of post-processing algorithms. For convenience we termed the spatial average of the Binning Statistics figure-of-merit as the Constellations Fitness value. Figures 9-13 show the plot of the fitness values for constellations consisting of 1, 2, 3, 4, and 5 Drone spacecraft respectively.

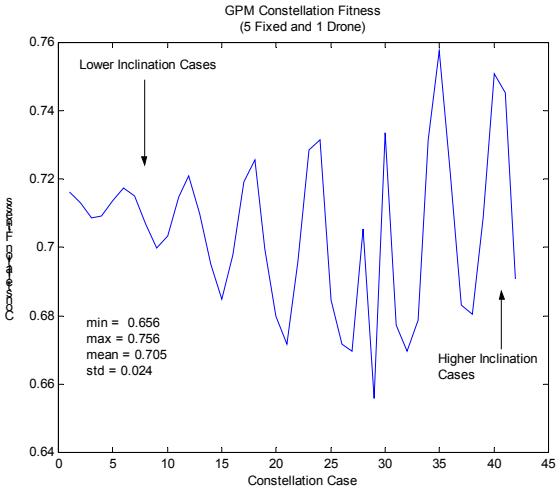

Fig. 9. Constellation Fitness for the 1 Drone Cases (42 Cases Examined).

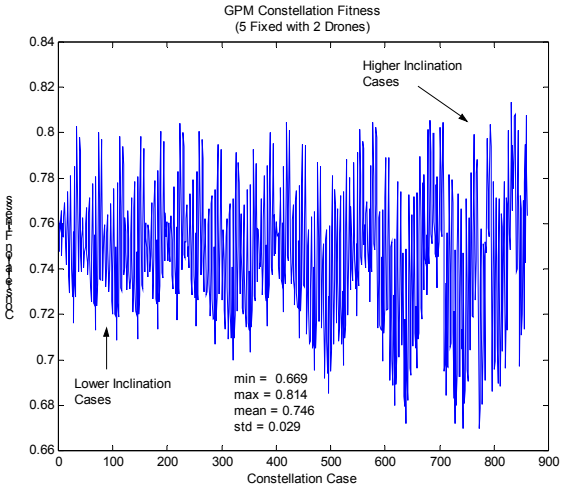

Fig. 10. Constellation Fitness for the 2 Drone Cases (861 Cases Examined).

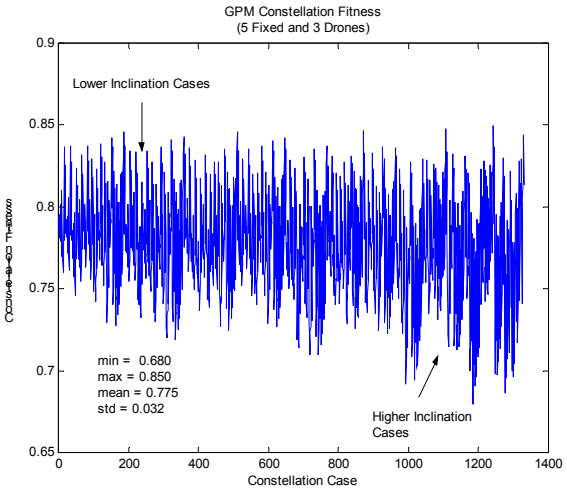

Fig. 11. Constellation Fitness for the 3 Drone Cases (1330 Cases Examined).

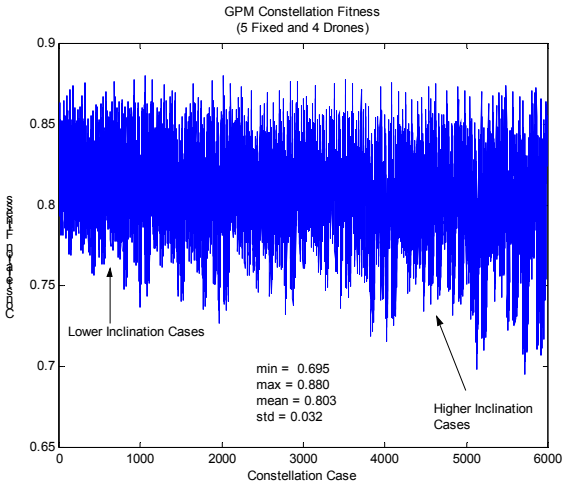

Fig. 12. Constellation Fitness for the 4 Drone Cases (5985 Cases Examined).

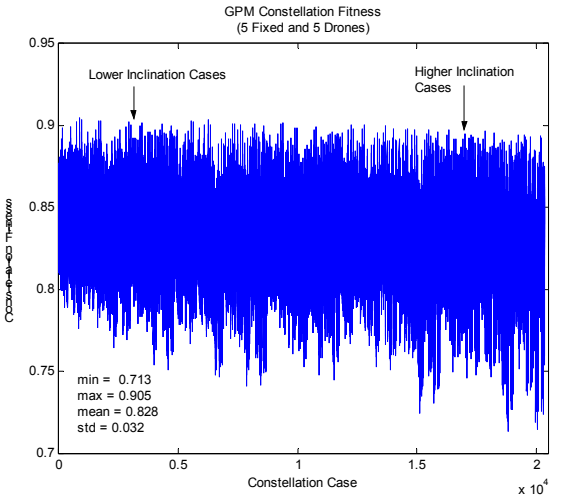

Fig. 13. Constellation Fitness for the 5 Drone Cases (20349 Cases Examined).

Figure 14 shows how the statistics associated with the Constellation Fitness grow as a function of the number of spacecraft.

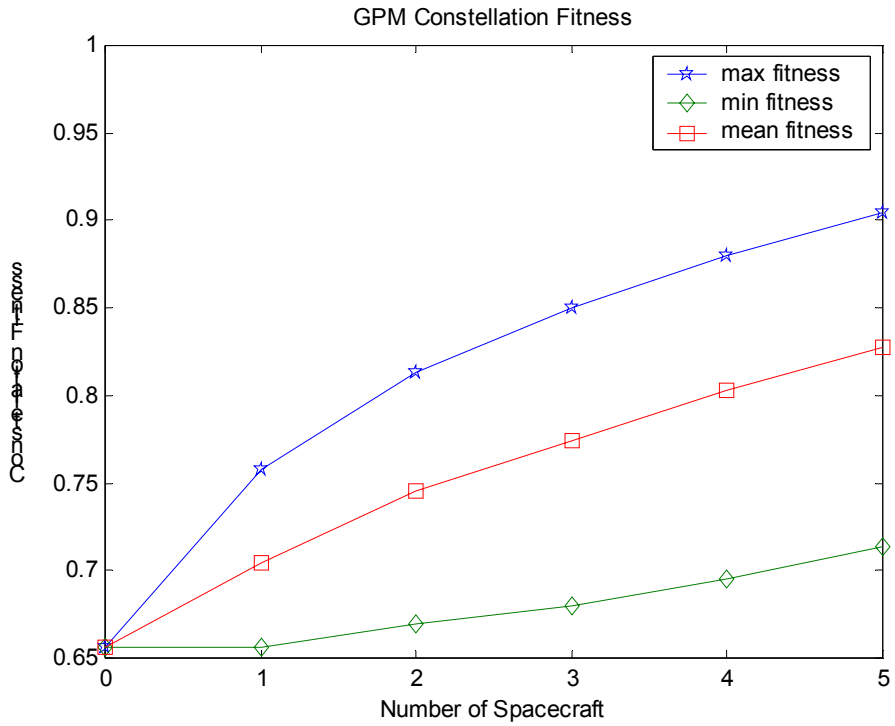

Fig. 14. Statistical Measures of the GPM Constellation Fitness as a Function of the Number of the Drones in the Constellation.

Table 6, shows the break down for the maximum in each constellation type according to the Drone spacecraft presented in Table 3.

Table 6. The Makeup of the Maximum Constellation Fitness Cases for Each Constellation Type.

Constellation Type	Maximum Constellation Fitness	Comprising Spacecraft
Fixed + 1 Drone	0.756	35
Fixed + 2 Drones	0.814	34, 41
Fixed + 3 Drones	0.850	23, 35, 41
Fixed + 4 Drones	0.880	1, 23, 35, 41
Fixed + 5 Drones	0.905	1, 3, 23, 35, 41

Finally, Figure 15 shows histograms for each constellation type. As can be seen from the figure, in each constellation type approximately 2.5 percent of the cases are at or near the maximum fitness value.

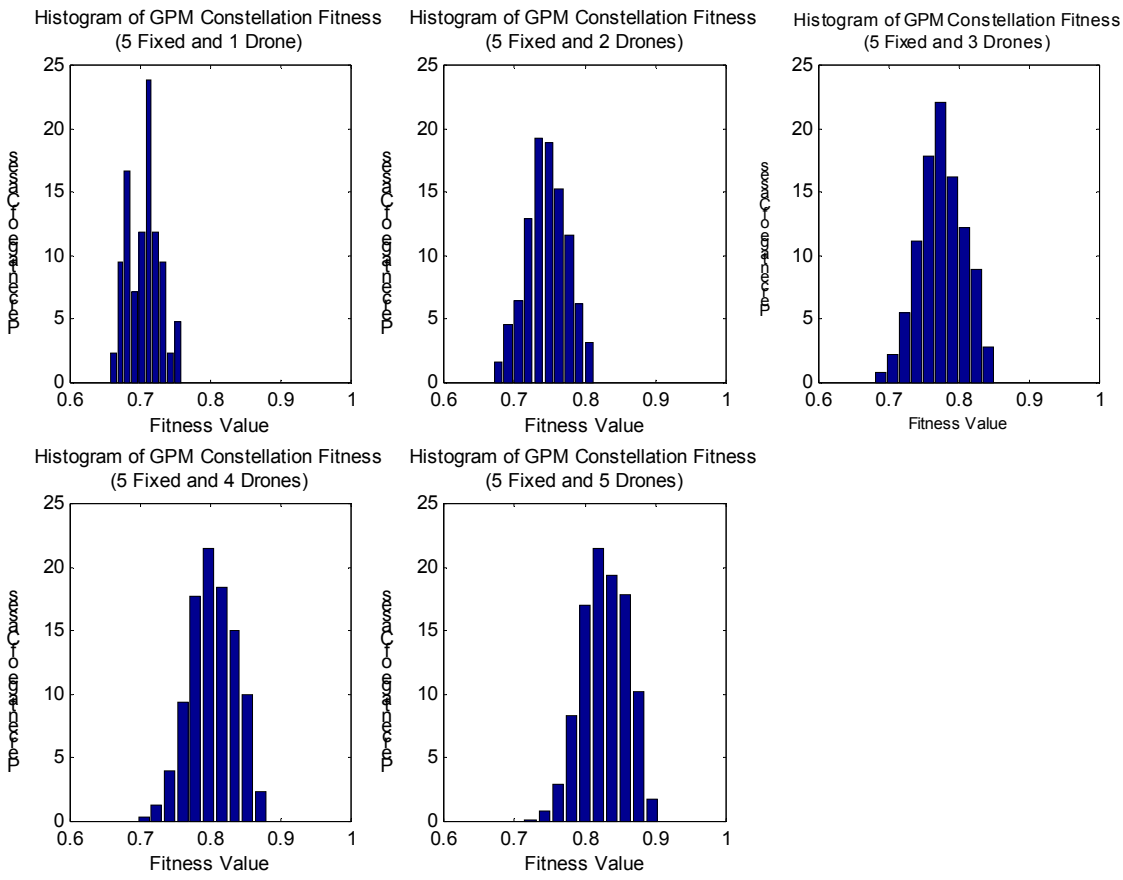

Fig. 15. Histograms for Each of the Constellation Types. Top row from left to right: 5 Fixed + 1 Drone, 5 Fixed + 2 Drones, and 5-Fixed + 3. Bottom row from left to right: 5 Fixed + 4 Drones and 5 Fixed + 5 Drones. Note that many constellation configurations yielded Binning Statistics near the maximum.

We found, using this metric that there were many combinations of spacecraft that gave fitness values at or near the maximum. In addition, these cases were distributed over the different inclinations and nodes (see Figure 9-13).

Sun-Synchronous Drones

Building on the observation from the previous analysis that the high inclination cases seem to provide the better Constellation Fitness, the next analysis performed centered on Sun-Synchronous Drones. The basic reason for this restriction is that since three of the five Fixed spacecraft are Sun-Synchronous then perhaps better results would be obtained if the Drones themselves had identical nodal regression rates. Again using ***FreeFlyer®***, two sets of 36 spacecraft were propagated for 15 days with a 60-second step size using a J_2 force-model. Separate Binning Statistics were again kept for each spacecraft over each of the 15 days, with 8 bins per day, giving a total of 120 bins. The number of points used in the coverage model was 5000. The data was generated in ***FreeFlyer®***, in approximately 3.7 hours, and was collected in Matlab®. The resulting data was just over 300 megabytes.

The 72 Drone spacecraft were all given the orbital elements detailed in Table 7. The inclination was chosen so that they were Sun-Synchronous. The 72 Drones were further divided into two classes. The first 36 spacecraft had right-ascension of the ascending nodes ranging from 0° to 350° in steps of 10° and

true anomalies of 0° (Drone class 1). The second 36 spacecraft had the same node spacing but started with true anomalies of 180° (Drone class 2). In addition, the Drones were assigned a cone half-angle of 43.2°.

Table 7. Orbital elements common to all Drone spacecraft.

Drone Orbital Element	Value
alt.	600 km
E	0
I	97.7876°
ω	0°
F	0° (Drone class 1) or 180° (Drone class 2)

Once the ***FreeFlyer®*** run was completed, different GPM constellations were examined. Each constellation consisted of the 5 Fixed spacecraft plus between 1 and 2 Drones. The various cases are shown in Table 8.

Table 8. GPM Constellation runs.

Constellation Type	Number of Possible Cases	Number of Examined Cases	Approximate Computing Time (PII 500MHz)
Fixed + 1 Drone (Class 1)	36	36	1 min
Fixed + 1 Drone (Class 2)	36	36	1 min
Fixed + 2 Drones (1 from each Class)	1296	1296	20 min

Again, in order to make the results more manageable, the Constellation Fitness, discussed above, was employed. Figures 16-17 show the plot of the fitness values for constellations consisting of 1 Drone spacecraft from either Drone class 1 or Drone class 2.

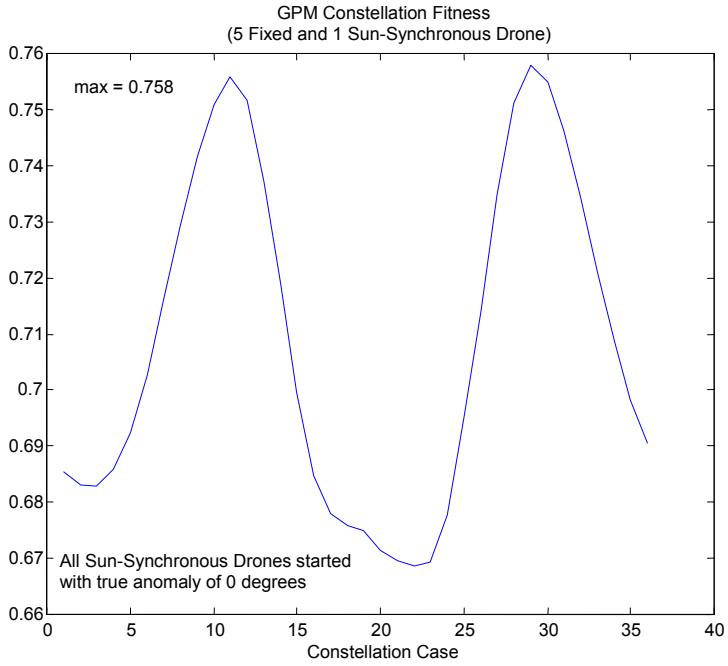

Fig. 16. Constellation fitness for the 1 Drone cases (Drone class 1).

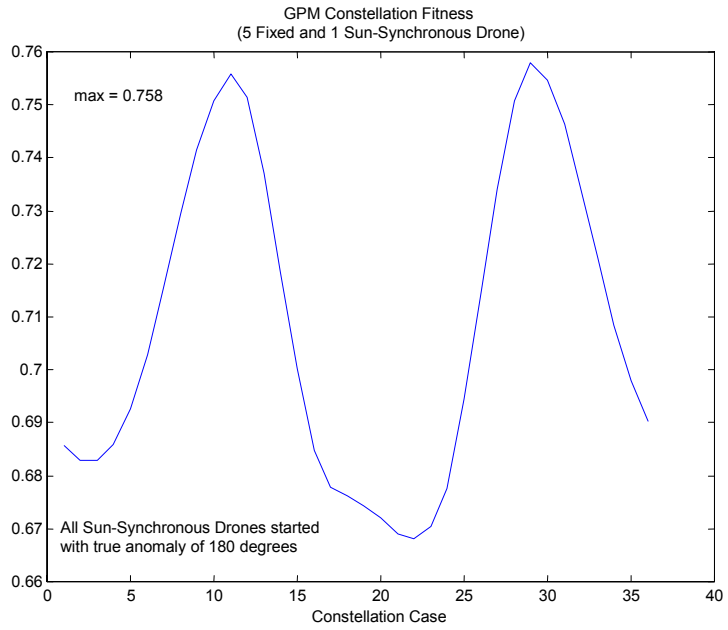

Fig. 17. Constellation fitness for the 1 Drone cases (Drone class 2).

It is clear from these figures that the true anomaly does not play a role for the 1 spacecraft case. The maximum Constellation Fitness, in both figures, obtains for cases 11 or equivalently 29, corresponding to a right-ascension of ascending node of 110 or 290 degrees or a mean-local-time of 2:42 pm or 2:42 am. Figure 18, shows the Constellation Fitness values for all possible 7 spacecraft constellations comprised of the 5 Fixed spacecraft plus 2 Drone spacecraft, one from Drone class 1 and one from Drone class 2.

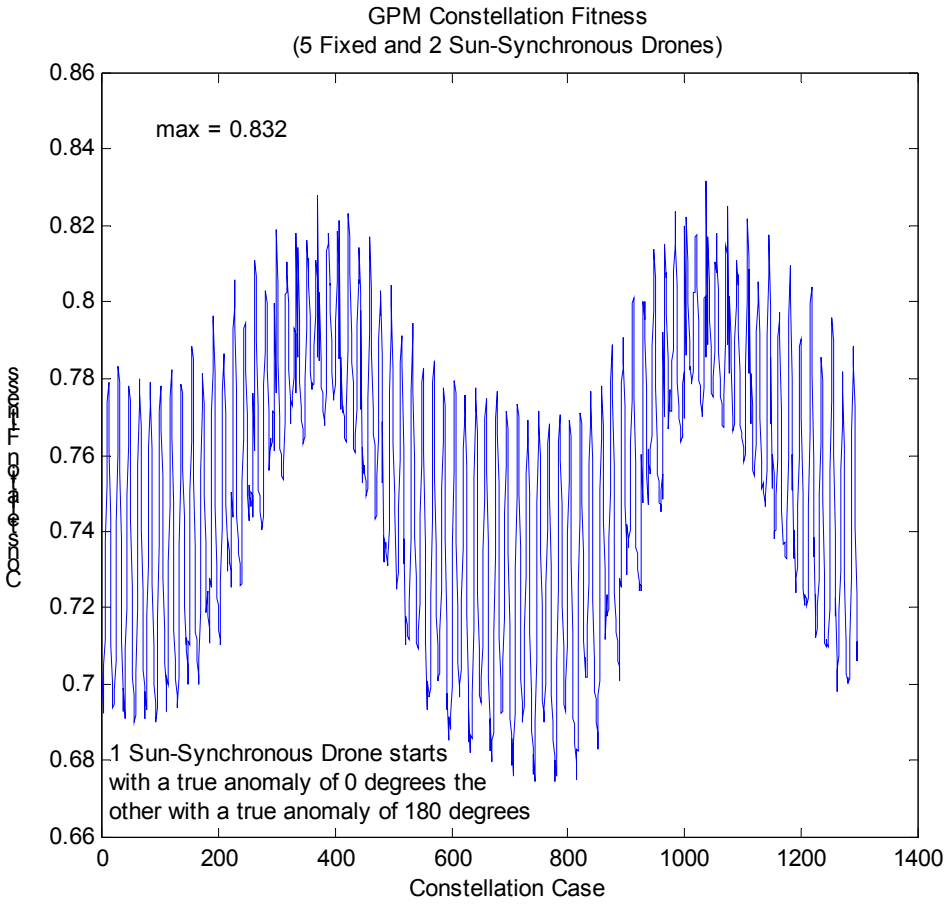

Fig. 18. Constellation fitness for the 2 Drone cases (1 from Drone class and one from Drone class 2).

The maximum fitness of the 2-Drone constellation was obtained with case 11 (or equivalently case 29, since the two are related by a 180 degree shift in true anomaly) at a Constellation Fitness value of 0.832. We draw this portion of the analysis to a close by comparing these results with the results from the analysis with the Arbitrary Drones presented:

- The 1 spacecraft case resulting in the maximum Constellation Fitness had a node of 120 degrees, an inclination of 95 degrees, and a fitness value of 0.756 in the previous analysis. The corresponding data for this analysis are a node of 110 degrees, an inclination of 97.78 degrees, and a fitness value of 0.758.
- The 2 spacecraft case resulting in the maximum Constellation Fitness had nodes of 90 and 120 degrees and had inclinations of 85 and 95 degrees, in the previous analysis. The corresponding fitness value was 0.814. The corresponding data for this analysis were nodes at 100 and 110 degrees and inclinations at 97.78 degrees. The corresponding fitness value was 0.832.

Long-Term Constellation Evolution

In this section, we present the work performed on the long-term evolution of the Constellation. To gauge the long term evolution, we used ***FreeFlyer®*** to produce a time series of the spatial average of the 3-hour Coverage figure-of-merit for an entire year. The Constellation Fitness used above (*i..e.* the spatial average of the Binning Statistics) is then obtained by an appropriate moving average. Figure 19, shows

the long-term behavior for a constellation comprised solely of the Fixed spacecraft. In general, the data trend is essentially flat with an average of about 0.68 and fluctuations that have excursions as high as 0.73 and as low as 0.62.

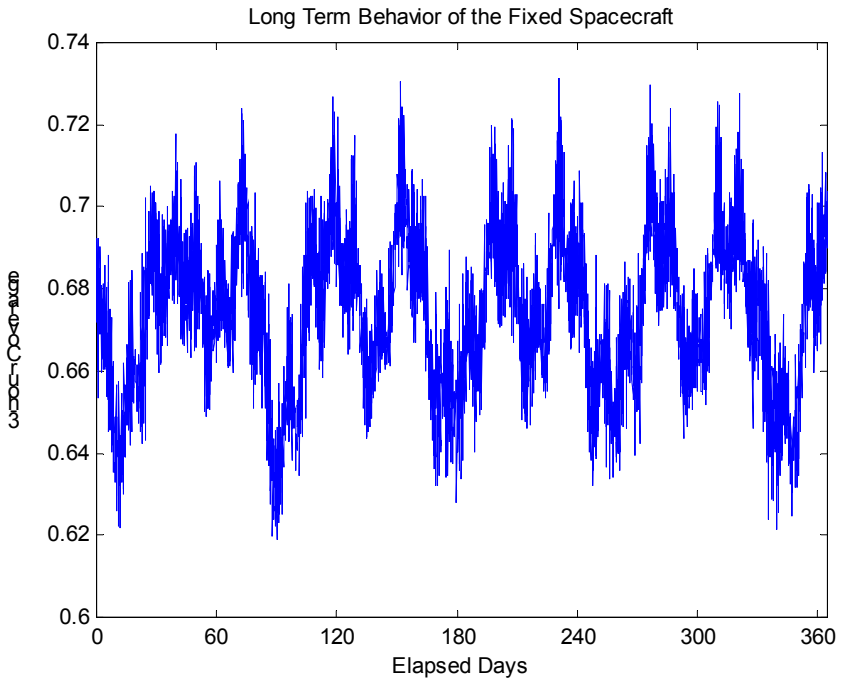

Fig. 19. Long-term behavior of the 3-hour Coverage of the Fixed spacecraft over 1 year. The Constellation Fitness (i.e. the spatial average of the Binning Statistics) are obtained by taking the appropriate moving average).

Consistent with the above results (see Figure 14), as more spacecraft are added, the 3-hour Coverage rises. However, the long-term evolution can show signs of secular trends. Consider the four constellation cases shown in Figure 20(a-d). For convenience, we will specify the free orbital elements of the Drones in the compact notation (a,b,c) where the values for a, b, and c will be the inclination, right-ascension of the ascending node, and the true anomaly (in degrees) respectively. In Case (a), the constellation is comprised of Drones with elements (95,110,0), (95,110, 180), (35,0,0). This case was constructed by combining the Fixed spacecraft with the best two Sun-Synchronous Drones and then scanning over the Arbitrary Drones to find the best fit. Then the inclinations were backed off of their Sun-Synchronous values and the long-term evolution was performed. The results obtained were suggestive of the role of J_2 was playing. Although the 3-hour Coverage initially increased, the trend quickly reached a maximum and then fell. The same case was run without the J_2 term in the force model and the results are shown in Figure 20(b). Here the trend of the 3-hour Coverage remained relatively flat with a maximum not quite as high as obtained in Case (a) but with a minimum well above the minimum of Case (a). Although we need to perform more analysis, we believe that these results suggest that only Sun-Synchronous Drones can achieve long-term stability as their nodal regression rates match those of most of the Fixed spacecraft. This conjecture seems also to explain why the trend in Case (a) is first "increase" then "decrease". If the nodal rates of the Drones are not matched to the Sun-Synchronous members of the Fixed, then the relative spacing between the nodes changes in time. This change has the effect of moving the constellation configuration along the curves shown in Figures 9-13. Thus a constellation configuration that has yielded a high value for the 3-hour Coverage over a period of time (i.e. a high value for the Constellation Fitness)

will eventually transition to configuration with a low value. Further evidence comes by comparing Cases (c) and (d). In Case (c) the Drones have free orbital elements given by (95,110,0), (95,110,180), (95,0,0). In Case (d) the Drones have the same orbital elements as in (c) with the exception that the inclinations were now set to their Sun-Synchronous values. Comparing the two plots shows clearly how the trend in Case (c) is to first increase and then decrease while the same plot for Case (d) remains essentially flat.

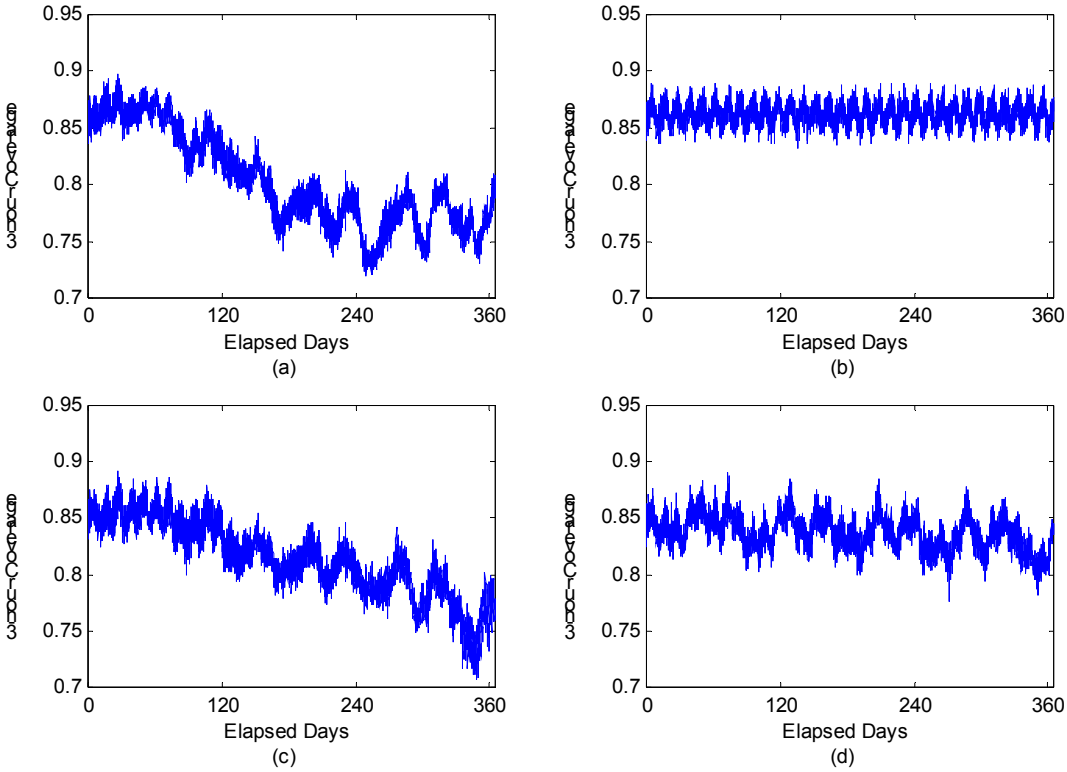

Fig. 20. Long-term behavior of a variety of GPM constellations comprised of the Fixed spacecraft and 3 Drones. Using the notation (a,b,c) to denote the Drone's inclination, right-ascension of the ascending node, and true anomaly (in degress) the cases are as follows. Case a) the Drones are at (95, 110,0), (95,110,180), and (35,0,0). Case b) is the same as case a) but with no J_2 term in the force model. Case c) the Drones are at (95,100,0), (95,110,180), and (95,0,0). Case d) is similar to case c) with the exception that the inclinations were chosen to be Sun-Synchronous.

Genetic Algorithm

As mentioned earlier, the computationally intense nature of the scanning for increasing number of spacecraft in the constellation restricted the analysis to part of the solution space. Consequently, a genetic algorithm (GA) seemed a natural transition from our "brute-force" search. Genetic algorithms are particularly efficient methods for finding a solution in a large space of possible solutions. The GA evaluates, according to a fitness criteria, which members of an initial set of solutions (i.e. initial population) to keep or to discard. Then, new members are added to the population by reproduction or mutation of the "good" members of the population following a stochastic process. This elimination/reproduction-mutation cycle is repeated for N iterations or until the best member of the population reaches a desired fitness value.

The results presented in this section were generated using the Matlab genetic search toolbox from Optimal Synthesis [5] to optimize the ***FreeFlyer®*** data used above. For this analysis, we defined two fitness criteria labeled "pure fitness" and "mixed fitness". The "pure fitness" refers to the spatial average

of the Binning Statistics figure-of-merit defined in the previous section. The "mixed fitness" is defined as the "pure fitness" minus the spatial standard deviation of the temporal average of the Binning Statistics. This second figure-of-merit was introduced to evaluate the spatial uniformity of the average Binning Statistics. For the GA runs, we used the 42 drones from Table 3. In addition, the GPM-Core and Megha-Tropiques (MT) right-ascension of the ascending node were allowed to vary between 0 and 150 degrees by increment of 30 degree corresponding to 6 additional spacecraft each. DMPS-F18, DMSP-F19 and GCOMB1 shown in Table 1 remained unchanged. Binning Statistics were recorded for a total of 57 spacecraft for 7 days with a 60-second step size using a J_2 force-model.

Each chromosome or member of the population was coded as a sequence of case number. The first two numbers represent MT and the GPM-Core respectively. Each of the following number represents an additional drone picked from the 42 cases. For example, when considering 3 additional drones, a constellation coded as: '2 6 12 41 28' translate to the constellation detailed in Table 9.

Table 9. Constellation Orbital Elements Corresponding to the Chromosome '2 6 12 41 28'

Orbital Element or Parameter	DMSP-F18	DMSP-F19	GCOMB1	Megha-Tropiques	GPM-Core	Drone 1	Drone 2	Drone 3
alt (km)	833	833	803	867	400	600	600	600
e	0	0	0	0	0	0	0	0
i (deg)	98.748	98.748	98.620	22	65	45	95	75
Ω (deg)	152.03	197.03	227.28	30	150	150	120	90
ω (deg)	0	0	0	0	0	0	0	0
f (deg)	0	0	0	0	0	0	0	0
swath width (km)	1707	1707	1600	1600	920	1600	1600	1600
swath alt. (km)	833	833	803	800	400	800	800	800
half-angle (deg)	43.715	43.715	43.085	43.186	47.81	43.186	43.186	43.186

**shaded areas represent varied orbital elements or parameters.*

An initial population of 214 members was generated for each run. When creating a population, one has to make sure that all the possible cases are present so as not to remove possible solutions from the search space. Thus, the 200 first members were generated randomly and the remaining 14 were manually implemented to ensure that all the possible 54 cases were included. The run was stopped after 1500 iterations and the population was restricted to a maximum of 500 members. New members were added with a 70% probability of crossover with randomly selected parents and 30% of mutation with randomized selection of a parent based on fitness. When the population reached its maximum, the 'worst' fitness candidates were decimated. For each of the fitness studied, the best candidate's orbital elements and its corresponding 7-days spatial average Binning Statistic plot are presented. In addition, a preliminary long-term analysis of the solutions is provided. The constellations presented below are composed of 8 spacecraft (i.e. 3 additional drones).

Results

As shown in Table 10 the best "Pure Fitness" constellation, with a fitness of 0.859, seems to favor higher inclinations. This result is in agreement with the maximum fitness value found using the scanning

method in the section above. As mentioned previously, we do not currently have a science-derived figure-of-merit. Thus we shouldn't expect that the constellation can be evaluated solely on the fitness value used before, and so the spatial distribution of the Binning Statistics was also analyzed (Figure 21) along with the long-term behavior of the 3-hour coverage (Figure 22). The point we wish to emphasize, is that the spatial averaging, which formed the heart of the scanning methods, is likely failing to capture important details vital to successful science. Our hope is that the GA approach will allow us to work more of the spatial structure of the Binning Statistics into consideration without causing an undue computational strain. Looking at Figure 21, we notice that high latitudes have the highest score of average Binning Statistics with about 0.9 (i.e. 90% of the total 56 bins hit in average). The lowest fitness is located in the ±35-50 deg latitude band and is about .75 and .80. This result appears inadequate for GPM, which defines its zone of interest within the ±70 deg latitude band. The highest fitness score is mainly concentrated out of the target area. In addition, the long-term temporal average of the cumulated coverage seen in Figure 21 slopes down as time elapses. This result suggests that the solution generated using such a short time-span (7 days) is not temporally stable under J_2 perturbation.

Table 10. Best Candidate Inclination and Right Ascension of the Ascending Node (Pure Fitness)

	MT	GPM-Core	D1	D2	D3
i (deg)	22	65	85	95	35
Ω (deg)	150	150	90	120	90

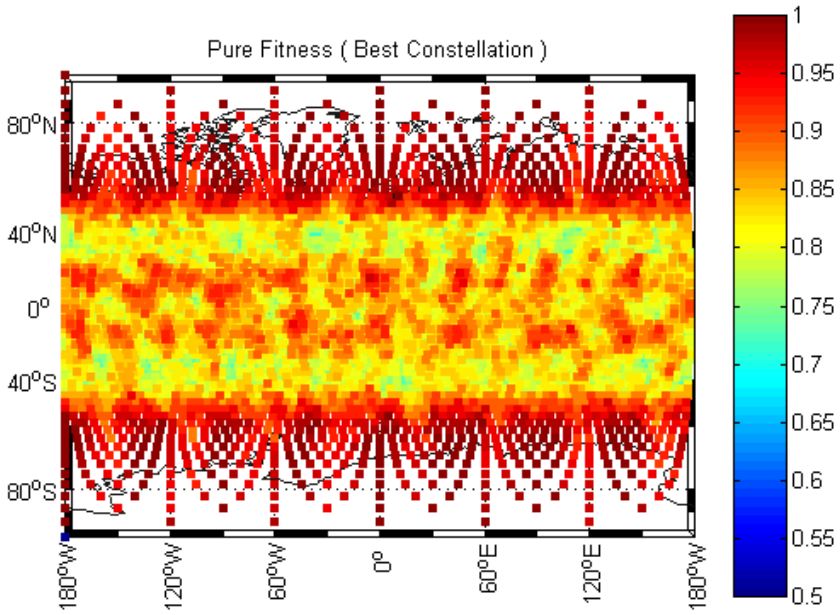

Fig. 21. 7-Days Average Binning Statistics Plot (Pure Fitness)

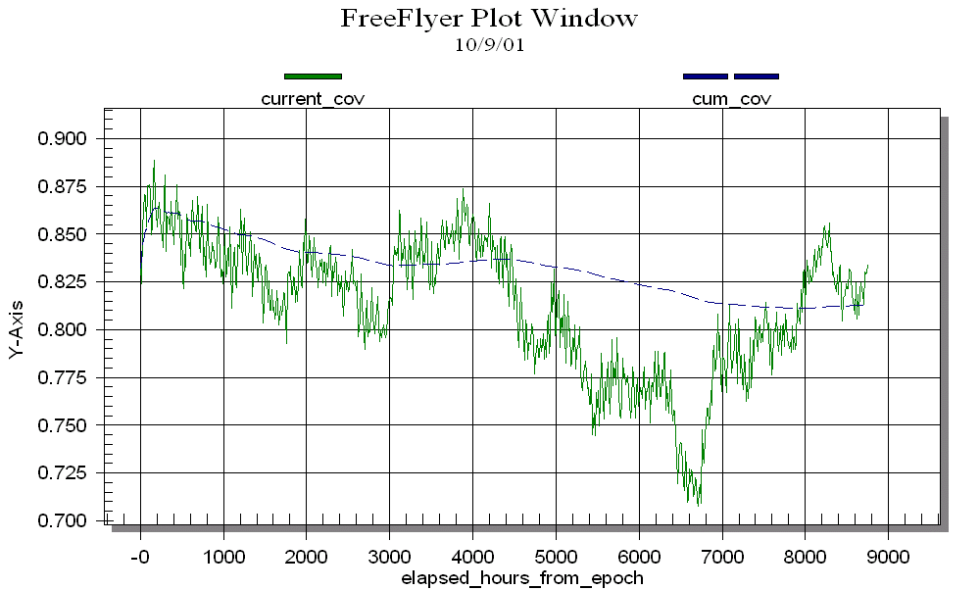

Fig. 22. Yearly Coverage Variation (in Green) and Cumulated Average Coverage (in Blue) using a "Pure Fitness" Criteria.

To distribute the Binning Statistics more uniformly, another fitness value (i.e. "mixed fitness") which penalizes high spatial standard deviation is introduced. The new constellation shown in Table 11 now favors lower inclinations with a fitness of .8473. Even though the fitness value is lower than the previous solution, we observe a better distribution of the Binning Statistics as a function of latitude in Figure 23. Finally, while this modification improves the solution by 'smoothing-out' the spatial distribution, the long-term behavior (see Figure 24) again suffers the same falloff as other constellations with low-inclination Drones (Figure 20-c).

Table 11. Inclination and Right Ascension of the Ascending Node (Mixed Fitness)

	MT	Core	D1	D2	D3
i (deg)	22	65	55	35	95
Ω (deg)	120	90	150	30	90

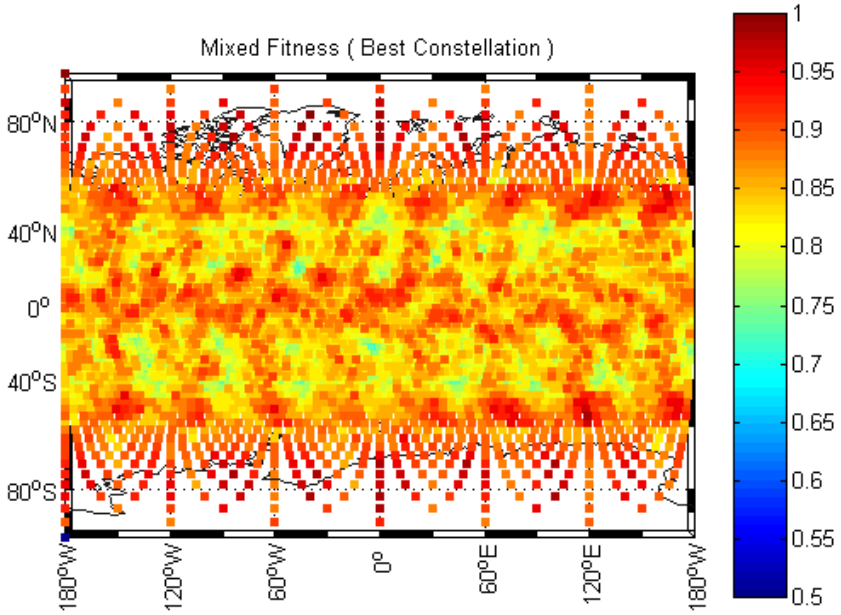

Fig. 23. 7-Days Average Binning Statistics Plot (Mixed Fitness)

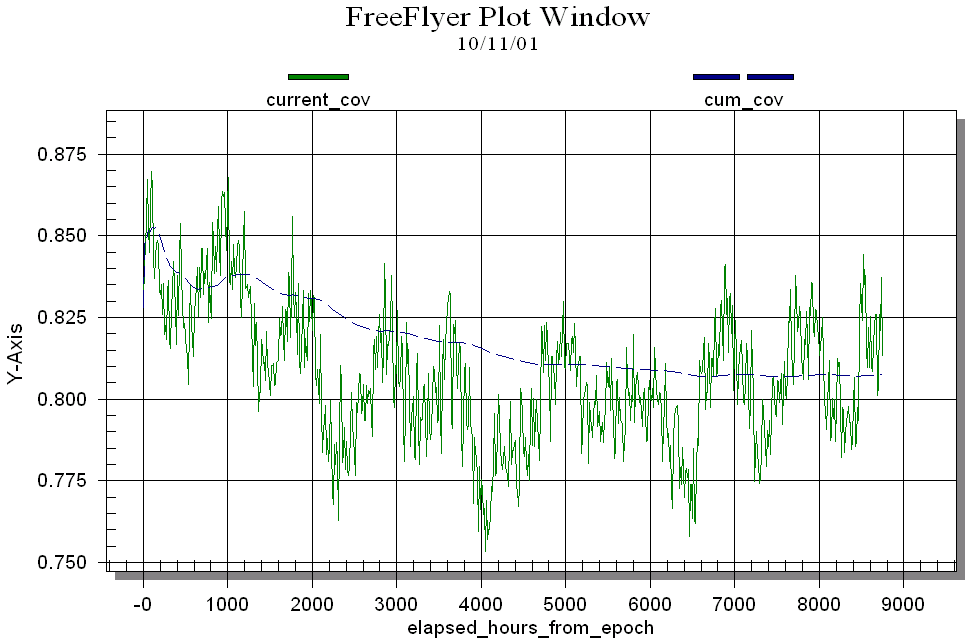

Fig. 24. Yearly Coverage Variation and Cumulated Average Coverage (Mixed Fitness)

In conclusion, the fitness defined for the preliminary GA runs is not adequate to generate a stable long-term solution. Attempts to achieve a uniformly spatial distribution of the Binning Statistics was successful by implementing a "mixed fitness" which took into account the spatial standard deviation of the "pure fitness". Therefore, we envision that spatially-averaged snapshots of the "mixed fitness",

sampled for, perhaps, 3 days once per month, might be a better figure-of-merit to capture the complexity of the solution.

CONCLUSIONS

This paper summarizes our preliminary efforts in designing the Global Precipitation Measurement (GPM) constellation. GPM hybrid constellation mixes shared resources (Fixed spacecraft) along with GPM-specific drones. Our first goal was to best design the placement of the complementary spacecraft to satisfy mission requirements. The first figure-of-merit merit investigated is the global 3-hour coverage between ±70 deg. However, additional figures-of-merit were considered such as Revisit Statistics and Binning Statistics and evaluated in terms of the GPM science goals. The Binning Statistics were chosen as our main figure-of-merit for the bulk of our results as they appeared the best trade-off between accuracy and computing time. To build intuition on the problem we developed Indra/COV, a standalone Matlab tool. This visualization produced by Indra/COV was essential in advancing our understanding of the spatial characteristics of the figures-of-merit we were investigating. However, the plots produced were not amenable to an automated optimization scheme. Thus we moved to a ***FreeFlyer®***/Matlab® functionality, which allowed us to generate a database of 15-day Binning Statistics compiling each candidate spacecraft. The GPM constellation design thus transformed into solving a combinatorial problem (*i.e.* find the combination of drone that would lead to the best figure-of-merit). We first looked into scanning over the possible spacecraft combinations where the constellations were composed of the 5 Fixed spacecraft and some mix of either the Arbitrary or the Sun-Synchronous Drones. However, as the number of combinations grew with the number of spacecraft, scanning all possible combinations quickly became prohibitive without leaving out part of the solution space and we thus moved to a genetic algorithm (GA). Our preliminary results from the GA suggest that lower inclination Drones lead to a more uniform spatial average of the Binning Statistics. However, when considering the long-term stability, the Sun-Synchronous Drones appear as a better solution. Indeed, because the Fixed spacecraft are already Sun-Synchronous, the initially designed average 15-day Binning Statistics is maintained under J_2. On the other hand, we observed that Sun-synchronous drones exhibit high fitness in the high latitude band which are of little interest to GPM mission. Our future work will focus on working closely with the GPM project scientists to develop a combine coverage/rain fall model. We would like to determine how important the temporal and spatial fluctuations in the coverage are to the accurate measurement of precipitation. This study would allow us to construct a fitness criteria better tailored to the GPM needs. Along with search for new figure-of-merit, we also need to further analyze the effects of perturbations other than J_2. Finally, our efforts will continue on developing the GA method as it has generated results in agreement with the scanning method for significantly smaller fraction of computing time.

REFERENCES

[1] The GPM Project Website, http://gpm.gsfc.nasa.gov/

[2] M. Belló Mora, J. P. Muñoz, and G. Dutruel-Lecohier, "ORION – A Constellation Mission Analysis Tool",

[3] The Mathematical Atlas, http://www.math-atlas.org/index/spheres.html

[4] G. Klitsch, et. al., "Flight Dynamics Distributed (FDDS) Generalized Support Software (GSS) Functional Specification, Volume 1: Core Software", GSFC Technical Document 553-FDD-93/046R1UD5

[5] Optimal Synthesis, Inc., "Genetic Search Toolbox".